

EXTRACELLULAR BIOSYNTHESIS, CHARACTERIZATION AND CYTOTOXIC EFFECTS OF ZINC OXIDE NANOPARTICLES SYNTHESIZED FROM THE SUPERNATANT OF PROBIOTIC BACTERIUM, *BACILLUS AMYLOLIQUEFACIENS* CS4

Nobel surya pandi durai R, Arul D, Aiswarya D, Perumal P

Abstract: The present investigation focuses on the biosynthesis and characterization of zinc oxide nanoparticles (ZnO NPs) using cell free supernatant (CFS) of *Bacillus amyloliquefaciens* CS4 and evaluation of their anticancer and antioxidant properties. The ZnO NPs were characterized by X-ray diffraction (XRD), electron transmission microscope (TEM) and atomic force microscope (AFM). The TEM and AFM images revealed the biosynthesized ZnO NPs were in the size range of 4-16 nm and found to be spherical in shape. The ZnO NPs exhibited cytotoxicity on HeLa cell line with the effective half maximal inhibitory concentration (IC₅₀) value of 74.23 µg/mL. The DPPH results showed significant (P<0.05) antioxidant activity by ZnO NPs with an IC₅₀ value of 86.38 µg/mL. Furthermore, brine shrimp toxicity assay of ZnO NPs revealed half maximal lethal concentration (LC₅₀) value of 133.78 µg/mL on *Artemia salina*. The synthesized ZnO NPs have caused potential cytotoxic effects on HeLa cells and antioxidant activity and it could be used for cancer drugs development.

Keyword: *Bacillus amyloliquefaciens*, zinc oxide nanoparticles, anticancer, antioxidant, toxicity assay.

1 INTRODUCTION

Biological methods of nanoparticle synthesis using bacteria have offered an ecologically friendly and reliable alternative to chemical and physical methods [1]. The bacteria and fungi are naturally been bestowed with the property of reducing/oxidizing metal ions into metallic/oxide nanoparticles and thereby functioning as mini nanofactories [2]. The development of reliable, harmless, and eco-friendly methods for the synthesis of nanoparticles are the most important to increase their biomedical applications. So the best options to achieve this goal are to use the microorganisms to synthesize nanoparticles [3]. Among metal oxide Nanoparticles, ZnO have many significant features such as chemical and physical stability, high catalysis and effective antibacterial activity [4]. The ZnO NPs are one of the multifunctional inorganic nanoparticles that have many features like intensive ultraviolet and infrared adsorption properties with various applications [5]. Biodegradability and low toxicity are the most important characteristic features of ZnO nanomaterials [6]. Remarkably, the researchers have found the non-toxic nature of ZnO NPs to human cells and they hold good biocompatibility to human cells. Previously, several microorganisms have been reported for extracellular synthesis of ZnO nanoparticles *viz*, *Bacillus cereus* [7], *Lactobacillus plantarum* [8], *Rhodococcus pyridinivorans* [9] and *Lactobacillus* spp. [10].

The non-targeted organisms like zebrafish embryo and *Artemia* are generally considered to be of experimental models to test the toxicity of different NPs [11]. Among several biomedical applications, the use of ZnO NPs in cancer has been well explored. Published studies have revealed that ZnO NPs has strong pharmacological properties such as anti-cancer, antimicrobial and antioxidant activities [12-13]. Hence, the present investigation focuses on the *B. amyloliquefaciens* CS4 mediated synthesis of zinc oxide nanoparticles (ZnO NPs), the spectral characterization of the synthesized NPs and evaluation of their cytotoxic and antioxidant potential.

2 MATERIALS AND METHODS

2.1 Strain isolation and culture condition

The potential probiotic strain, *B. amyloliquefaciens* CS4 was previously isolated from the gut of snake head fish (*Channa striata*), and identified by 16S rRNA sequencing which was submitted on gene bank database (Genbank accession no. MK326902.1). Stock culture was maintained in sterile LB broth containing 20% (v/v) glycerol at 70°C and subculture was taken from the stock and then used for nanoparticle synthesis.

2.2 Preparation of cell free supernatants (CSF)

The LB broth was prepared and sterilized, and then 0.5 ml of fresh culture of *B. amyloliquefaciens* CS4 was inoculated and the medium was incubated for 48 h at 37°C. After the incubation period, the broth culture was centrifuged at 8,000 rpm and their supernatant was collected and the supernatant used for nanoparticle synthesis.

2.3 Extracellular synthesis of zinc oxide nanoparticles

The extracellular ZnO nanoparticle synthesis was carried out by adopting the method of Selvarajan *et al.* (2013) [8]. The zinc sulphate (5mM) was added to the flask containing 100 ml supernatant and heated up to 70°C for 10 min on a water bath and incubated for 24 h at 37°C. The white precipitate formed

- Department of Biotechnology, School of Biosciences, Periyar University, Salem, Tamil Nadu, India, 636 011 Corresponding Author: perumalarticles@gmail.com

at the bottom of the flask indicates the reduction process and the white precipitate collected by centrifugation at 10,000 rpm for 10 min. The precipitated ZnO nanoparticles were washed with deionized water and ethanol, then dried at 40°C and solid of ZnO NPs was collected. The powdered ZnO NPs sample was further analyzed by different characterization techniques.

2.4 X-ray diffraction (XRD) pattern

The synthesized ZnO NPs were subjected to X-ray diffraction analysis to determine the crystal structure, size and chemical composition. During XRD analysis, the spectrum was recorded in Rigaku Miniflex II, Japan advance X-ray diffractometer, operated at a voltage of 40 kV, in which the sample was subjected to Cu radiations at 4 min speed at a drive axis of 2 θ . Further, the values obtained were compared with the Joint Committee on Powder Diffraction Standards (JCPDS) library to determine the particle crystalline structure.

2.4 Transmission Electron Microscope

The size and morphology of the ZnO NPs was determined using Transmission Electron Microscope (TEM). The ZnO nanoparticles were diluted and a drop was coated on the copper grid and allowed to dry. The micrographs of the NPs were taken using TEM at 80 kV (TECHNA110, Philips, Netherland).

2.5 Atomic force microscope (AFM)

AFM analysis of the NPs were performed using an Agilent 5500 atomic force microscope with silicon cantilever model All-In-One-AI, manufactured by Budget Sensors with spring constant and typical resonance frequency 2.7 N/m and 80 kHz, respectively, and tip radius.

2.6 Antioxidant assay

DPPH radical is scavenged by antioxidants through the donation of a proton forming the reduced DPPH. Various concentrations of the sample (4.0 ml) were mixed with 1.0 ml of solution containing DPPH radicals, resulting in the final concentration of DPPH being 0.2 mM. The mixture were shaken vigorously and left to stand for 30 min, and the absorbance was measured at 517 nm. Ascorbic acid was used as control. The percentage of inhibition in DPPH radical scavenging activity was calculated using formula,

$$\% \text{ DPPH (inhibition)} = \frac{A_0 - A_1}{A_0} \times 100$$

Where A_0 is control, A_1 is sample.

2.7 MTT assay for cytotoxicity assessment

HeLa cell lines were cultured in Dulbecco's Modified Eagle's Medium (DMEM-Sigma) supplemented with 10% fetal bovine serum (Sigma) and antibiotic solution. Cells (1000 cells/ml) were seeded into 96-well plates containing 100 μ l of DMEM and maintained in a humidified, 5% CO₂ incubator at 37°C. After 24 h of incubation, the synthesized nanoparticles at different concentrations (12.5, 25, 50, 75, 100 μ g/mL) were dispersed in distilled water and added to each well and incubated for 24 and 48 h, to study the effect of concentration of ZnO NPs and exposure time in cell viability. Control cells received the same amount of the diluent (distilled water). Each test was performed in triplicate to check the sensitivity. After the completion of the exposure period (24 and 48 h) the medium in each well was replaced by fresh medium (100 μ l) containing 5 mg/mL of MTT (3-(4, 5-dimethylthiazol-2-yl)-2,5-diphenyltetrazolium bromide, Sigma). Subsequent to four

hours of incubation at dark, the formazan crystal of MTT reduction was dissolved in DMSO and absorbance was measured using a microtitre plate ELISA reader (BioTek). The effect of ZnO nanoparticles was quantified as the percentage of control absorbance of reduced MTT dye at 570 nm. Viability of the cells was assessed by the ability of living cells to reduce the yellow dye MTT to a blue formazan crystal. The percentage of cell viability was calculated by using the formula, % cell viability = (OD sample/OD control) \times 100 Where, OD is the optical density value.

2.8 Brine shrimp toxicity bioassay

The acute toxicity was determined by measuring the adverse effect of various concentrations of ZnO NPs on brine shrimp, *Artemia salina*. The lethality bioassay was performed using 25 nauplii for each concentration of the ZnO NPs, which was tested with varied concentrations viz, 0, 12.5, 25, 50, and 100 μ g/mL in artificial seawater and the assay was carried out in triplicate. The vials were maintained at room temperature for 24 h under the light and mortality of larvae was calculated, and their lethal concentration at 50 % (LC₅₀) was estimated using probit analysis.

3 RESULTS

3.1 Synthesis of ZnO nanoparticles

The extracellular synthesis of ZnO nanoparticles was initially confirmed by visual observation. By adding zinc sulphate with the *B. amyloliquefacians* CS4 culture filtrate, the precipitate formation was slowly observed after heating and the colour change was clearly indicates the nanoparticles formation (Fig.1). The formation of precipitate showed the occurrence of reaction between biochemical compounds in the supernatant and zinc sulphate that induced the development of zinc oxide nanoparticles.

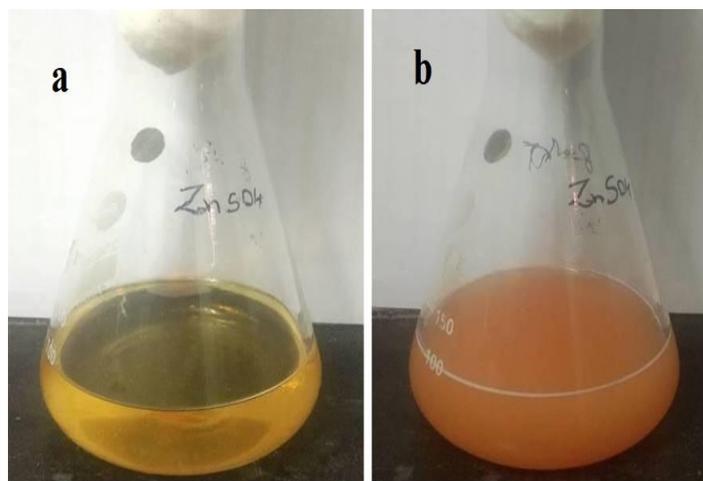


Fig. 1: Biosynthesis of ZnO nanoparticles: (a) culture supernatant, (b) addition of zinc sulphate after 24 h incubation

3.2 XRD pattern of Zinc oxide nanoparticles

The XRD profiles of the synthesized zinc oxide nanoparticles are shown in Fig. 2. The diffraction peak of synthesized zinc oxide nanoparticles exhibits 2 θ values at 12.46, 16.37, 21.86, 25.10, and 37.39 corresponding to the miller index (h k l) values as (200), (002), (111), (310), and (221) respectively,

which clearly indicate the formation of zinc crystalline nanoparticles. In the background of the graph is very clear maybe being due to the crystalline nature of the nanoparticles. The XRD pattern shows three intense peaks in the whole spectrum of 2θ values, that ranged between 20 and 40.

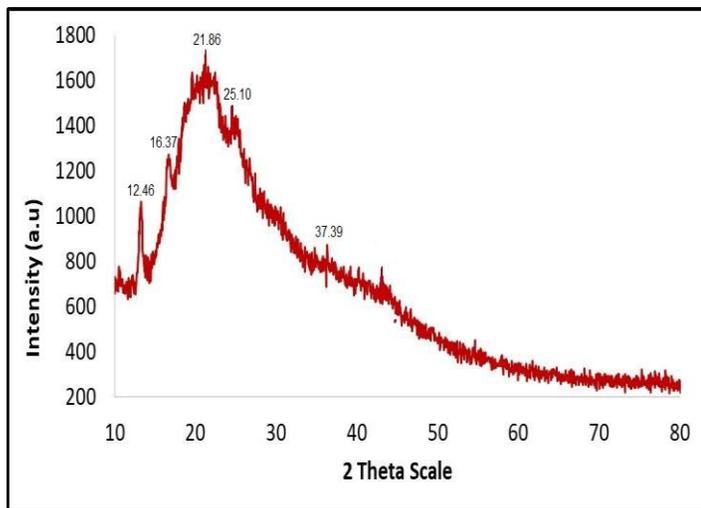


Fig. 2: XRD pattern of synthesized ZnO nanoparticles using CSF of *B. amyloliquefaciens* CS4

3.3 Transmission Electron Microscope (TEM)

The TEM images ZnO NPs revealed the spherical shape of particles with few number of aggregates (Fig.3) and the average size of the nanoparticles were in the range of 4 –16 nm. In the back ground of the nanoparticles some clumping like structure are there it may be the presence of bio chemicals in the bacterial supernatant.

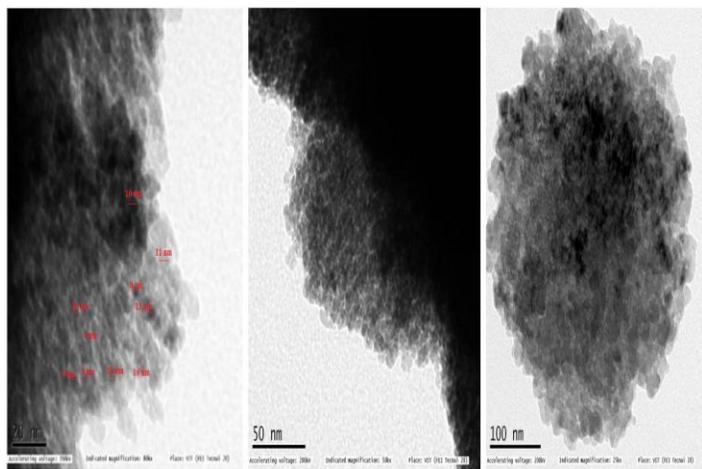


Fig. 3: Transmission electron microscope images of synthesized ZnO nanoparticles

3.4 Atomic Force Microscope (AFM)

The AFM analysis of synthesized ZnO NPs was carried out to assess their morphology and size range. The 2-D and 3-D images of AFM showed that most of the nanoparticles are spherical in shape and some of the agglomerations were present in the background of the nanoparticles (Fig. 4). The AFM images of nanoparticles morphology was inferred with TEM images.

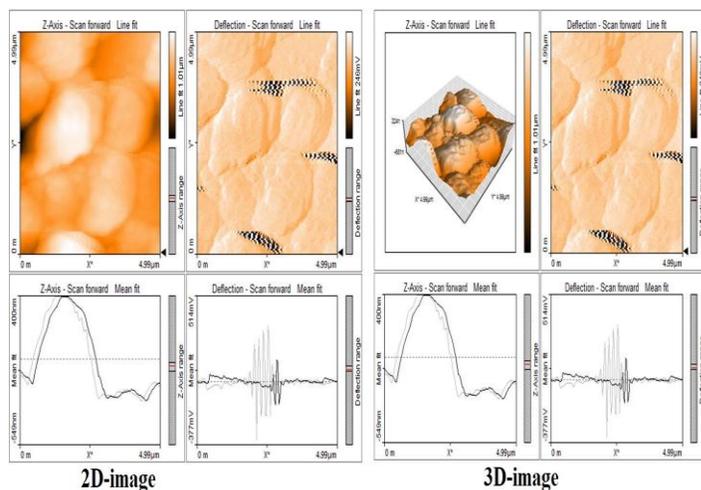


Fig. 4: AFM images of ZnO mediated by CSF of *B. amyloliquefaciens* CS4

3.5 MTT assay

The cytotoxic effect of ZnO NPs in HeLa cell line is graphically represented in Fig.5 and the treated cells were microscopically observed (Fig. 6). The obtained result infers an inverse relation between the NPs concentration and the cell viability. The half maximal inhibitory concentration (IC_{50}) was calculated from the graph with % viability and the IC_{50} value of ZnO NPs was found to be 74.23 $\mu\text{g/mL}$. the results demonstrated that treatment with ZnO NPs inhibited the growth of cells significantly ($P < 0.05$) and the cytotoxicity of the NPs is dose dependent.

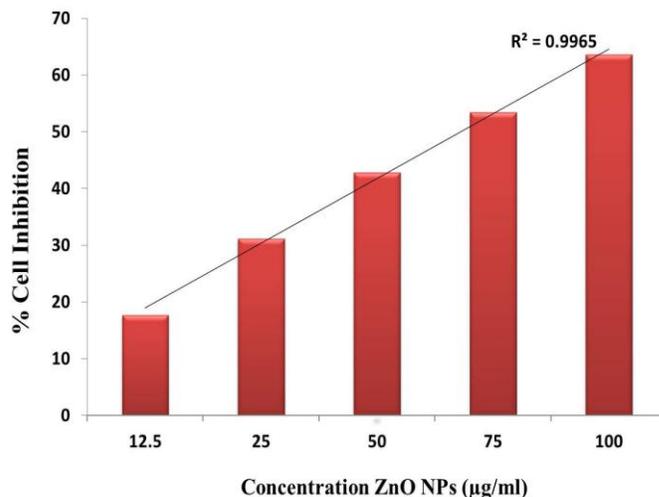


Fig. 5: Percentage of growth inhibition (MTT assay) of ZnO NPs against HeLa cells. ($IC_{50} = 74.23 \mu\text{g/mL}$, $R^2 = 0.996$).

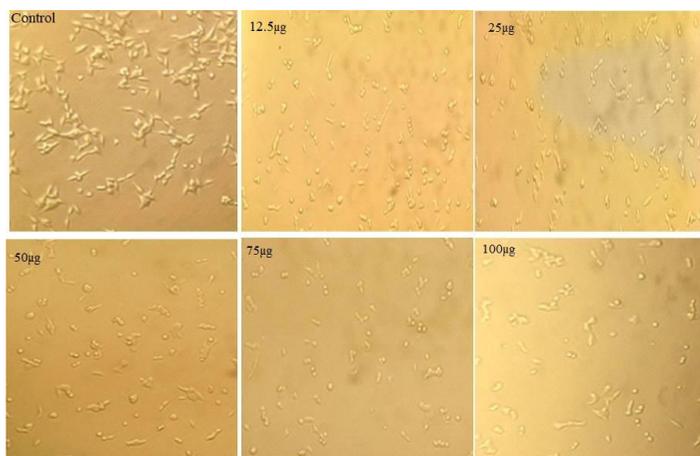


Fig. 6: Microscopic observation of ZnO NPs treated HeLa cells

3.6 Free radical scavenging activity-DPPH assay

The Antioxidant property of ZnO NPs was quantified spectrophotometrically by change in DPPH colour from purple to yellow and ascorbic acid used as standard. The percentages of inhibition of DPPH radical scavenging activity (RSA) are presented in Fig. 7. The DPPH results showed significant ($P < 0.05$) antioxidant activity by ZnO NPs from 10.40 to 54.20% for different concentrations. The radical scavenging activity was found to increase with the increased concentration of ZnO NPs showing the IC_{50} value of 86.38 $\mu\text{g/mL}$, with the positive control ascorbic acid showing IC_{50} value of 74.56 $\mu\text{g/mL}$.

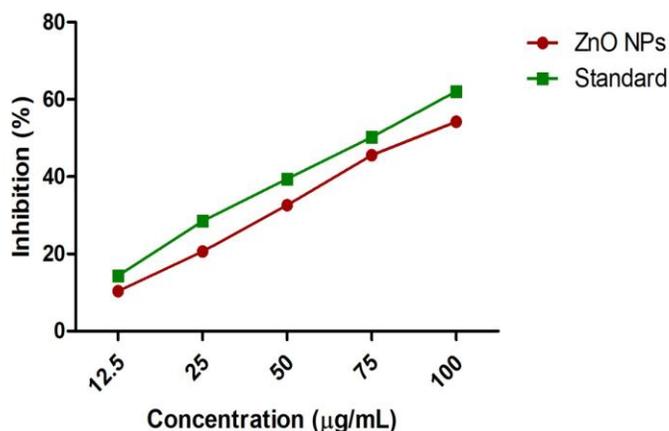


Fig. 7: DPPH radical scavenging activity of biosynthesized ZnO NPs (Standard-Vitamin C). The data are expressed as mean \pm SD ($n=3$).

3.7 Brine shrimp toxicity assay

The *Artemia* nauplii treated with different concentrations ZnO NPs and after 24 hours of treatment were observed under the phase contrast microscope and the results were photographed (Figs. 8). The mortality of *Artemia* larvae due to ZnO NPs is gradually increased with higher concentration of NPs. The control did not show any mortality after 24 h of incubation. At the minimum concentration (12.5 $\mu\text{g/mL}$), there was no mortality but during increase in concentration from 25, 50 and 100 $\mu\text{g/mL}$, the mortality was about 4.0, 13.3 and 30.6%, respectively. The lethal concentration values at 50% (LC_{50}) was calculated using Probit analysis (chi square not

significant, $P > 0.05\%$), LC_{50} value of ZnO NPs was found 133.78 $\mu\text{g/mL}$.

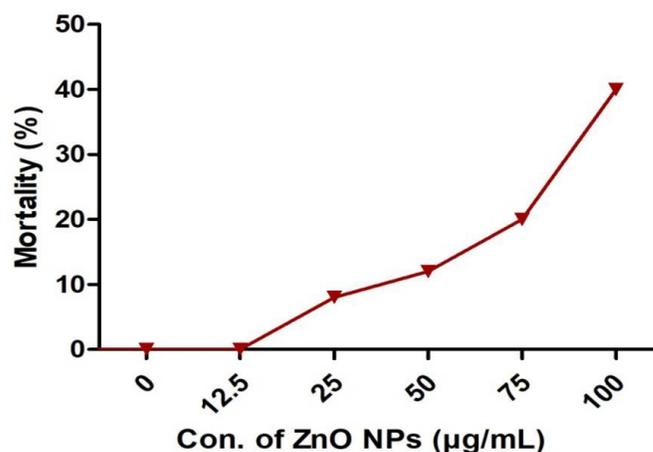
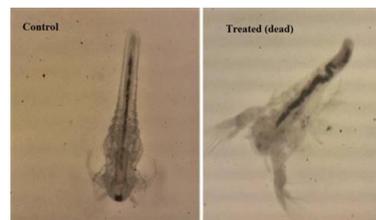


Fig. 8: Effect of different concentration of ZnO NPs on *A. salina* after 24 h treatment. Microscopic observation, the morphology of control and treated dead nauplii of *A. salina*.

4 DISCUSSION

Bacteria produce extracellular polymeric substances (EPS), that are the organic compounds comprising of polysaccharides, proteins, nucleic acids, lipids, and such compounds are reported to play crucial role in the bio-mediated synthesis of nanoparticles [14-15]. During recent past, many researchers have synthesized different nano particles from various bacteria and among them *Bacillus* species provide great openings for new discoveries [16-18]. Recently, Hatem Fouad *et al.* (2017) synthesized silver nanoparticles through the cell free supernatant of *B. subtilis* (A15) and *B. amyloliquefaciens* (D29), that exhibited strong activity against bacterial pathogens [16]. The XRD results confirmed that the synthesized ZnO nanoparticles were crystalline in nature with their peaks at 21.86 and 37.39 that can be indexed to the (1 1 1) and (2 2 1) set planes, respectively. Presently, the size of the produced nanoparticles were found diameter in the range of 4-16 nm that has been supported with the earlier findings of Selvarajan *et al.* (2013), who had synthesized ZnO NPs using probiotic bacteria *Lactobacillus plantarum* VITES07 that ranged between 7 and 17 nm [8]. The TEM and AFM analyses revealed that obtained nanoparticles were in a hexagonal, polydispersed, nearly spherical in shape. Earlier, Malarkodi *et al.* (2014) have synthesized zinc sulphide (ZnS) nanoparticles using *Klebsiella pneumoniae* and reported that the ZnS nanoparticles were spherical shaped and the size range of the nanoparticles was 10-25 nm [17]. Whereas, the *Aspergillus niger* synthesized ZnO NPs were in the size range of 84-91 nm [13]. Presently, free radical scavenging capacity of ZnO NPs were assessed

using DPPH assay, which showed scavenging activity with IC_{50} value of 74.66 $\mu\text{g/mL}$. Similarly, Murali *et al.* (2017) have reported antioxidant property of ZnO NPs that exhibited excellent free radical scavenging activity with an IC_{50} value of 95.09 $\mu\text{g/mL}$ [12]. Recently, ZnO NPs have gained considerable interest due to their potential against cancer cells. Presently, MTT assay ZnO nanoparticles exhibited potential toxic effect against HeLa cells showing IC_{50} value of 74.23 $\mu\text{g/mL}$. Previously, Kulkarni *et al.* (2016), who have reported cytotoxicity of ZnO nanoparticles against HeLa cell lines with IC_{50} value of 45.82 $\mu\text{g/mL}$ [18]. Earlier, Wahab *et al.* (2013) reported that ZnO NPs exhibited cytotoxicity on malignant human T98G gliomas, KB epidermoids and non-malignant normal HEK kidney cells [19]. The ZnO NPs revealed a good anticancer activity of against HeLa, HepG2 and MCF-7 cancer cells (MTT assay) [20]. Presently, the results of *Artemia* toxicity assay clearly demonstrated that the ZnO NPs were not acutely toxic to *Artemia* at low concentrations. The increased toxicity on *A. salina* could have been due to the prolonged exposure to elevated Zn^{2+} ions [21]. On the other hand, it has been reported that the mortality of *A. salina* increased significantly with increased concentrations of ZnO NPs [22]. The presently generated data based on the *B. amyloliquefaciens* CS4 extracellular synthesized ZnO nanoparticles and their biological properties have been of immense potential for further research.

REFERENCES

- [1] Narayanan KB, Sakthivel N. Biological synthesis of metal nanoparticles by microbes. *Advances in colloid and interface science*. 2010 Apr 22;156(1-2):1-3.
- [2] Kalpana VN, Devi Rajeswari V. A review on green synthesis, biomedical applications, and toxicity studies of ZnO NPs. *Bioinorganic chemistry and applications*. 2018 Feb: 1-12.
- [3] Nair B, Pradeep T. Coalescence of nanoclusters and formation of submicron crystallites assisted by *Lactobacillus* strains. *Crystal growth & design*. 2002 Jul 3;2(4):293-8.
- [4] Kalyani, G., V.G. Anil, C. Bo-Jung and L. Yong-Chien, 2006. Preparation and characterization of ZnO nanoparticles coated paper and its antibacterial activity study. *J. Green Chem.*, 8: 1034-1041.
- [5] Matei A, Cernica I, Cadar O, Roman C, Schiopu V. Synthesis and characterization of ZnO-polymer nanocomposites. *International Journal of Material Forming*. 2008 Apr 1;1(1):767-70.
- [6] Farzana R, Iqra P, Shafaq F, Sumaira S, Zakia K, Hunaiza T, Husna M. Antimicrobial behavior of Zinc oxide nanoparticles and β -lactam antibiotics against pathogenic Bacteria. *Arch. Clin. Microbiol.* 2017;8:57.
- [7] Hussein MZ, Azmin WH, Mustafa M, Yahaya AH. *Bacillus cereus* as a biotemplating agent for the synthesis of zinc oxide with raspberry-and plate-like structures. *Journal of inorganic biochemistry*. 2009 Aug 1;103(8):1145-50.
- [8] Selvarajan E, Mohanasrinivasan V. Biosynthesis and characterization of ZnO nanoparticles using *Lactobacillus plantarum* VITES07. *Materials Letters*. 2013 Dec 1;112:180-2.
- [9] Kundu D, Hazra C, Chatterjee A, Chaudhari A, Mishra S. Extracellular biosynthesis of zinc oxide nanoparticles using *Rhodococcus pyridinivorans* NT2: multifunctional textile finishing, biosafety evaluation and in vitro drug delivery in colon carcinoma. *Journal of photochemistry and photobiology B: Biology*. 2014 Nov 1;140:194-204.
- [10] Salman JA, Kadhim AA, Haider AJ. Effect of ZnO Nanoparticles Synthesized by *Lactobacillus gasseri* on Expression of CZC Genes in *Pseudomonas aeruginosa*. *Journal of Global Pharma Technology* 2018; 10(03):348-355.
- [11] Anitha R, Ramesh KV, Ravishankar TN, Kumar KS, Ramakrishnappa T. Cytotoxicity, antibacterial and antifungal activities of ZnO nanoparticles prepared by the *Artocarpus gomezianus* fruit mediated facile green combustion method. *Journal of Science: Advanced Materials and Devices*. 2018 Dec 1;3(4):440-51.
- [12] Murali M, Mahendra C, Rajashekar N, Sudarshana MS, Raveesha KA, Amruthesh KN. Antibacterial and antioxidant properties of biosynthesized zinc oxide nanoparticles from *Ceropegia candelabrum* L.—an endemic species. *Spectrochimica Acta Part A: Molecular and Biomolecular Spectroscopy*. 2017 May 15;179:104-9.
- [13] Safawo T, Sandeep BV, Pola S, Tadesse A. Synthesis and characterization of zinc oxide nanoparticles using tuber extract of anchote (*Coccinia abyssinica* (Lam.) Cong.) for antimicrobial and antioxidant activity assessment. *OpenNano*. 2018 Jan 1;3:56-63.
- [14] Sanghi R, Verma P. Biomimetic synthesis and characterisation of protein capped silver nanoparticles. *Bioresource technology*. 2009 Jan 1;100(1):501-4.
- [15] Padman AJ, Henderson J, Hodgson S, Rahman PK. Biomediated synthesis of silver nanoparticles using *Exiguobacterium mexicanum*. *Biotechnology letters*. 2014 Oct 1;36(10):2079-84.
- [16] Fouad H, Hongjie L, Yanmei D, Baoting Y, El-Shakh A, Abbas G, Jianchu M. Synthesis and characterization of silver nanoparticles using *Bacillus amyloliquefaciens* and *Bacillus subtilis* to control filarial vector *Culex pipiens pallens* and its antimicrobial activity. *Artificial cells, nanomedicine, and biotechnology*. 2017 Oct 3;45(7):1369-78.
- [17] Malarkodi C, Rajeshkumar S, Paulkumar K, Vanaja M, Gnanajobitha G, Annadurai G. Biosynthesis and antimicrobial activity of semiconductor nanoparticles against oral pathogens. *Bioinorganic chemistry and applications*. 2014;2014.
- [18] Kulkarni BD, Sultana S, Bora M, Dutta I, Paarakh PM, Basappa VA. In vitro Cytotoxicity Studies of Zn (Zinc) Nanoparticles Synthesized from *Abutilon indicum* L. against Human Cervical Cancer (HeLa) Cell Lines. *Pharmacognosy Journal*. 2016;8(2).
- [19] Wahab R, Siddiqui MA, Saquib Q, Dwivedi S, Ahmad J, Musarrat J, Al-Khedhairy AA, Shin HS. ZnO nanoparticles induced oxidative stress and apoptosis in HepG2 and MCF-7 cancer cells and their antibacterial activity. *Colloids and surfaces B: Biointerfaces*. 2014 May 1;117:267-76.
- [20] Sharma V, Anderson D, Dhawan A. Zinc oxide nanoparticles induce oxidative DNA damage and ROS-triggered mitochondria mediated apoptosis in

- human liver cells (HepG2). Apoptosis. 2012 Aug 1;17(8):852-70.
- [21] Ates M, Daniels J, Arslan Z, Farah IO, Rivera HF. Comparative evaluation of impact of Zn and ZnO nanoparticles on brine shrimp (*Artemia salina*) larvae: effects of particle size and solubility on toxicity. Environmental Science: Processes & Impacts. 2013;15(1):225-33.
- [22] Khoshnood R, Jaafarzadeh N, Jamili S, Farshchi P, Taghavi L. Acute toxicity of TiO₂, CuO and ZnO nanoparticles in brine shrimp, *Artemia franciscana*. Iranian Journal of Fisheries Sciences. 2017;16(4):1287-96.